

L.A. Cornish, M.B. Shongwe, B. Odera, J.K. Odusote, M.J. Witcomb, L.H. Chown, G.O. Rading, M.J. Papo

## UPDATE ON THE DEVELOPMENT OF PLATINUM-BASED ALLOYS FOR POTENTIAL HIGH-TEMPERATURE APPLICATIONS

- L.A. Cornish** DST/NRF Centre of Excellence in Strong Materials, hosted by the University of the Witwatersrand, South Africa; School of Chemical and Metallurgical Engineering, University of the Witwatersrand, South Africa; African Materials Science and Engineering Network (AMSEN): A Carnegie-IAS Network,
- M.B. Shongwe** DST/NRF Centre of Excellence in Strong Materials, hosted by the University of the Witwatersrand, South Africa; School of Chemical and Metallurgical Engineering, University of the Witwatersrand, South Africa
- B. Odera** DST/NRF Centre of Excellence in Strong Materials, hosted by the University of the Witwatersrand, South Africa; School of Chemical and Metallurgical Engineering, University of the Witwatersrand, South Africa
- J.K. Odusote** DST/NRF Centre of Excellence in Strong Materials, hosted by the University of the Witwatersrand, South Africa, School of Physics, University of the Witwatersrand, South Africa, Faculty of Engineering and Technology, Department of Mechanical Engineering, University of Ilorin, Ilorin, Nigeria
- M.J. Witcomb** DST/NRF Centre of Excellence in Strong Materials, hosted by the University of the Witwatersrand, South Africa; African Materials Science and Engineering Network (AMSEN): A Carnegie-IAS Network
- L.H. Chown** DST/NRF Centre of Excellence in Strong Materials, hosted by the University of the Witwatersrand, South Africa; School of Chemical and Metallurgical Engineering, University of the Witwatersrand, South Africa; African Materials Science and Engineering Network (AMSEN): A Carnegie-IAS Network
- G.O. Rading** African Materials Science and Engineering Network (AMSEN): A Carnegie-IAS Network, Department of Mechanical and Manufacturing Engineering, University of Nairobi, Nairobi, Kenya
- M.J. Papo** DST/NRF Centre of Excellence in Strong Materials, hosted by the University of the Witwatersrand, South Africa; Advanced Materials Division, Mintek, South Africa

## Abstract

Pt-based alloys for high-temperature applications in aggressive environments have been under development for over 10 years, and are targeted to be used as either as bulk, or as coatings. The alloys comprise Pt, Al, Cr, and Ru, and the microstructure has been improved by composition to a best possible analogue of the nickel-based superalloys, which these alloys could partially replace. This was necessary because the previous best alloy had a strengthening precipitate volume proportion of only approximately 40 vol.%, whereas the nickel-based superalloys have around 70 per cent, and a lower volume would mean that the strength would not be the best that could be obtained. The microstructures were assessed using electron microscopy, and have been related to the alloys' hardness values. The current microstructures are much more like those of NBSAs, with a high proportion of the strengthening  $\sim\text{Pt}_3\text{Al}$  precipitates. Since the samples have to be small (platinum is expensive), hardness has been used as an indication of strength. Nano-indentation studies showed that the hardness and Young's modulus were higher for  $\sim\text{Pt}_3\text{Al}$  than the (Pt) matrix.

More extensive oxidation studies have been undertaken on the previous optimum sample, and the effect of cooling rate after heat treatment has also been ascertained. In addition, the samples were studied after different heat treatment times, and cross-sections were made in order to characterize the alumina scale that formed. The oxide scales of Pt-11Al-3Cr-2Ru (at.%) up to 100 h exposure did not spall, and were at least as good as those of the ternary alloys. There was no discernable Al depletion zone in the substrate, although it could have been at a greater depth than thickness of the samples studied.

Further additions to the Pt-Al-Cr-Ru alloys have been studied, to increase the melting temperature as well as to reduce the platinum content without compromising the properties. Reduced platinum content would have the benefits of reduced density and cost. The target elements include vanadium and niobium, of which vanadium is of special interest, since it is a South African product. Before these additions could be made, phase equilibria studies were undertaken so that the maximum addition could be ascertained, and also to check any possible ternary phases, which could be deleterious. Work on the Pt-Al-V system revealed a ternary phase,  $\sim\text{V}_{27}\text{Pt}_{54}\text{Al}_{19}$  (at.%), which has a eutectic reaction with (Pt). The maximum V addition is likely to be around 15 at.%, otherwise  $\sim\text{Pt}_3\text{V}$  or the ternary phase will form, and not the required (Pt)/ $\sim\text{Pt}_3\text{Al}$  phases.

## Introduction

The Pt-based project has been running for many years, and was initially funded by the Platinum Development Initiative which comprised Anglo American Platinum, Lonmin, and Impala Platinum, and two LEAD grants from the Government<sup>1-7</sup>. Most of the work was done either at Mintek or the University of the Witwatersrand, with involvement from other South African universities such as the universities of Cape Town, Limpopo, and the Free State.

There were also parallel studies at Fachhochschule Jena and the University of Bayreuth, Germany<sup>8-12</sup>, with some collaborations<sup>13-15</sup>, as well as with the National Institute for Materials Science (NIMS), Japan<sup>16-17</sup>.

The rationale behind the work is that Ni-based superalloys (NBSAs) are reaching their temperature limit, and despite improvements with the higher-generation alloys, the improvements are slowing down, and the last 24 years have produced an increase of approximately 100°C<sup>18</sup>. There have already been improvements with design, using forced air-cooling, and huge benefits from using coatings, which have an insulating outer layer. Both of these techniques are expensive and can have disastrous effects if they fail, for example, if the coating fails locally. Thus, there has been a push to develop a totally new suite of materials, and platinum-based alloys are one possible solution. Platinum was selected because it has the same fcc structure as Ni, but a higher melting point<sup>19</sup>, similar chemistry, and better oxidation and corrosion resistance<sup>20</sup>. The earlier work has already shown that the same microstructure as the NBSAs could be attained, although the volume of the strengthening precipitate was much less<sup>1-7</sup>, and that the corrosion resistance was much better<sup>21</sup>. The work soon identified Pt-Al as the best system both for beneficial microstructures and for formation of the protecting alumina film, and ternary additions were studied. The best ternary alloys were Pt-Al-Cr and Pt-Al-Ru, and these were then combined<sup>5,22</sup>. The target temperature of the Pt-based alloys is 1300°C, which is about 200°C higher than the currently-used NBSAs, and the optimum composition was Pt-11Al-3Cr-2Ru (at.%). The effect of heat treatment was studied<sup>3-7</sup>. However, the problems of the high expense and density remained.

In 2007, the study split, with work on coatings ongoing at Mintek<sup>23</sup>, and the more fundamental investigations continuing at the University of the Witwatersrand. This is an update on that work, and shows that there has been progress on both alloying to potentially reduce the proportion of expensive and dense platinum, and improving the microstructure to increase the proportion of the strengthening precipitates. Also, more work has been done on the oxidation of the alloys at high temperature, showing that the platinum-based alloys have good potential in aggressive environments through the formation of a stable and tenacious alumina film.

### **Improving the microstructure**

The NBSAs obtain their strength from the high proportion of ~Ni<sub>3</sub>Al precipitates in a (Ni) matrix. The precipitates have an ordered fcc structure and so the interface between the precipitates and the matrix has low interfacial energy, meaning that the driving force for coarsening is low, and hence the fine structure can be retained to relatively high temperatures<sup>4</sup>.

The Pt-based alloys have also been shown to have nearly the same structure, although there is a complication, because unlike in the Ni-Al system, the Pt-Al system has at least three different structures for the ~Pt<sub>3</sub>Al precipitates<sup>25-26</sup>, and the cubic high-temperature form is the preferred one. It can be stabilized by additions of Ti, Cr, and Ta<sup>16, 27</sup>.

The worst problem was that all the studies indicated that despite attempted to optimize the heat treatment, the highest precipitate proportion attained was around 30 per cent. Although the mechanical properties were promising<sup>28-30</sup>, obviously with such a small proportion of the strengthening precipitates, the alloys would not achieve their potential strength. The ruthenium additions were for both increased corrosion resistance as well as for solid-solution strengthening.

Studies of six alloy compositions in the as-cast and heat-treated states, and hardness tests, identified a new optimum composition: Pt-11Al-6Cr-5Ru (at.%), on the basis of a higher volume of the fine precipitates and increased hardness<sup>31-33</sup>. The casting was done in a button-arc melter under an argon atmosphere, with titanium used as an oxygen getter, and the heat treatment conditions were taken from the work on Pt-Al-Cr-Ni alloys<sup>8, 13</sup>: heat treated in air at 1500°C for 18 hours, then water-quenched, followed by 1100°C for 120 hours and air cooling. Furthermore, this particular heat treatment is more similar to current industrial practices for NBSAs, compared to the much longer times used in earlier work<sup>1-7</sup>. A study of the misfit, obtained from XRD, showed that the degree of misfit was related to shape of the precipitates<sup>34</sup>, just as in NBSAs<sup>24</sup>.

Using alloys around the new optimum composition of Pt-11Al-6Cr-5Ru (at.%), samples of approximately 3 g were manufactured by button-arc melting, then heat treated as above. Sections of approximately 250 µm were cut from the centre of the button, and 3 µm diameter cores were cut from these and then prepared as transmission electron microscope (TEM) samples<sup>35</sup>, with the final thinning being done on a Gatan 691 Precision Ion Polishing System (PIPS), with a final milling done at a lower energy and for a short time to reduce the ion damage. However, the ion damage was not sufficiently removed, and the method of Witcomb had to be utilized<sup>36</sup>. The samples were immersed in a solution made up of equal amounts of phosphoric, nitric and sulphuric acids at 2.8V AC at 20°C, with the sample positioned between two Pt electrodes. The cleaning time was about 30s<sup>36</sup>, and afterwards, the microstructures of ~Pt<sub>3</sub>Al precipitates in the (Pt) matrix were clearly seen.

The microstructure had much higher proportions of the ~Pt<sub>3</sub>Al precipitates<sup>35</sup> than in earlier studies<sup>1-7, 8, 13</sup>, and were comparable to the NBSAs (Figure 1). The average size of the precipitates was 200 nm. The morphology of the current precipitates was more cubic, and thus more similar to NBSAs than those in earlier work. The matrix was less easily removed and protruded more, showing that it was more resilient to the thinning. Electron diffraction patterns were obtained from several areas of the precipitates and the matrix by tilting, and the angles and distances were measured between the spots. The results were compared to the XRD results from the same samples to deduce the structures<sup>35, 37-39</sup>, by comparing different sets of *hkl* values. The different comparisons showed that the precipitates were more likely to be cubic than tetragonal, although some precipitates were more difficult to identify conclusively.

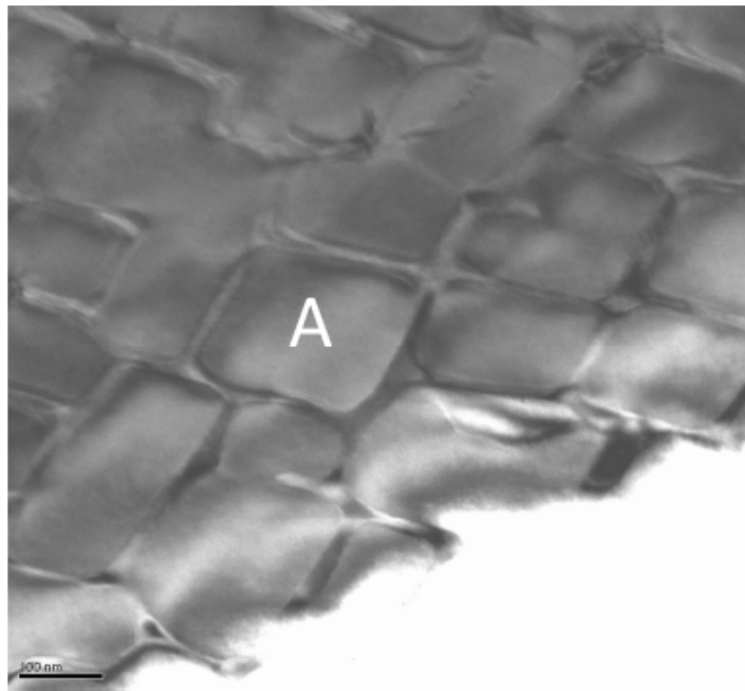


**Figure 1–TEM micrograph for nominal Pt-12Al-Cr4-Ru2 (at.%) showing  $\sim$ Pt<sub>3</sub>Al (marked A) with channels of (Pt) matrix [35]**

The nanohardness and the elastic (Young's) modulus were analysed on the separate phases of nominal Pt-12Al-Cr4-Ru2 (at.%) using a CSM nano-indenter with a maximum load of 2.5 mN. Ten individual indentations were averaged for determining the hardness and modulus of elasticity of the matrix and precipitates. The nanohardness results were  $11.4 \pm 0.9$  GPa for  $\sim$ Pt<sub>3</sub>Al, and  $7.3 \pm 0.6$  GPa for (Pt). Similarly, the elastic (Young's) modulus values were  $259.7 \pm 23.7$  for  $\sim$ Pt<sub>3</sub>Al and  $233.3 \pm 21.8$  for (Pt). The  $\sim$ Pt<sub>3</sub>Al values were higher than the matrix, as expected. Durst *et al.*<sup>40</sup> performed nanoindentation on the third-generation CMSX-10 NBSAs, and found the nanohardness to be 9.4 GPa for the  $\gamma'$ -precipitates and 7.2 GPa for the matrix, with an elastic modulus of 255 GPa for  $\gamma'$  and 231 GPa for  $\gamma$ . The  $\gamma'$ -phase in CMSX-10 is softer compared to that of Pt-12Al-Cr4-Ru2, while the matrix nanohardnesses are similar. Similar elastic modulus values were observed for both phases in CMSX-10 and Pt-12Al-Cr4-Ru2. The  $\gamma'$  and  $\gamma$  nanohardnesses of Pt-12Al-Cr4-Ru2 were similar to that of Pt-12Al-6Cr-5Ni-2Re<sup>41</sup>, which were 11.5 GPa for  $\gamma'$  and 7.5 GPa for  $\gamma$ . The elastic modulus for  $\gamma'$  was slightly lower compared to the 282 GPa of Pt-12Al-6Cr-5Ni-2Re, while the  $\gamma$ -phase elastic modulus of Pt-12Al-Cr4-Ru2 was slightly higher than that of Pt-12Al-6Cr-5Ni-2Re.

## Oxidation studies

Obviously, if alloys are targeted to be utilized in a fuel-burning environment, the reactions with oxygen and other deleterious components in the fuel have to be known.

Earlier studies had already shown the Pt-based alloy's superior corrosion resistance over NBSAs<sup>21</sup>, as well as good alumina scale-forming capabilities of the Pt-Al-Cr and Pt-Al-Ru ternary alloys between 1150°C and 1350°C<sup>42-43</sup>, after the formation of a discontinuous oxide layer during an initial transient stage of up to 10 hours. A continuous  $\alpha$ -Al<sub>2</sub>O<sub>3</sub> scale with no zone of discontinuous oxide or any internal oxidation was formed on Pt-14Al-3Cr-3Ru isothermally oxidized in air at 1350°C up to 500 hours<sup>44</sup>, but there were concerns that the scale formed too quickly, which might not be sustainable in long-term service. Wenderoth *et al.*<sup>12</sup> also observed the parabolic formation of alumina scale on a Pt-12Al-6Cr-5Ni (at.%) alloy when isothermally oxidized in air at temperature between 1100°C and 1300°C for up to 400 hours, and the Al depletion zone in the substrate increased with oxidation time and temperature. A more in-depth study was necessary to study how the alumina formed over time.

As-cast (button-arc melted) Pt-11Al-3Cr-2Ru (at.%) samples were heat-treated at 1350°C for 96 hours in a muffle furnace, then cooled in either water or air<sup>45</sup>. Approximately 1 mm thick slices were cut and prepared metallographically on both sides to a 1  $\mu$ m diamond finish. Isothermal oxidation tests were done in air at 1350°C for up to 100 hours. Specimens were removed after specific time intervals from 1 hour to 100 hours, and weighed after cooling. Specimens were prepared metallographically for cross-sectional examination using a SEM<sup>45</sup>.

The specific mass gain for each specimen in both quenching media increased parabolically (Figure 2) with exposure time, with the oxidation rate of the air-cooled specimens increasing faster<sup>45</sup>. There was no mass loss over the entire 100 hours' exposure at 1350°C, indicating good oxidation resistance, and no scale spallation. Although the higher oxidation rate of the air-cooled samples could be due partially to the additional oxidation that occurred while the samples were cooling, there is also the effect of available aluminium. The scale on the air-cooled specimens had potentially better adhesion than that on the water-quenched specimens, based on deeper protrusions of the scales into the substrate. This was a result of faster scale growth rates, leading to increased scale thicknesses. Both the mass- and thickness-related parabolic constants of the air-cooled specimens had higher scale growth rate constants than those of Süß *et al.*<sup>43</sup>, which may be due to a slightly higher Al content of the quaternary alloy, as well as beneficial effects of other alloying elements. Vorberg *et al.*<sup>9</sup> showed that Pt-12.5Al-3Cr-6Ni (at.%) quenched in water after heat-treatment at 1500°C contained small  $\gamma'$  precipitates with a volume fraction of about 3 per cent, whereas air-cooled samples were found to contain evenly-distributed cuboid-shaped  $\gamma'$  precipitates, with a volume fraction of approximately 30 per cent. The faster scale growth kinetics of the air-cooled specimens may be due to a higher volume fraction of  $\gamma'$  in the as-cast alloy.

Here, the microstructure of the air-cooled specimens could not be resolved, but the Al content was lower, which would be expected to result in a lower volume fraction of  $\gamma'$ . In both studies, the air-cooled specimens had thicker scales. One reason for thicker scale could be more free Al, but this was not true for the current alloys.

Another reason could be more  $\gamma'$  ( $\sim\text{Pt}_3\text{Al}$ ) precipitates, which would give more available Al for the scale. Vorberg *et al.*<sup>9</sup> reported the depletion of Al near the surface was due to the depletion of  $\gamma'$  precipitates.

This showed that the Al in the scale originated from the  $\gamma'$  precipitates, so it is likely that the air-cooled specimens had more  $\gamma'$  precipitates, especially since Pt-7Al-5Cr-3Ru (at.%)<sup>4</sup> had approximately 30 per cent precipitates by volume. These alloys have four components, so the proportion of  $\gamma'$  ( $\sim\text{Pt}_3\text{Al}$ ) precipitates might not be directly proportional to the Al content, since Al is present in both  $\sim\text{Pt}_3\text{Al}$  and (Pt) matrix. The faster scale kinetics of the air-cooled specimens, resulting in thicker scales, might have resulted from more  $\sim\text{Pt}_3\text{Al}$  in those samples. Mass-parabolic rate constants,  $k_p$ , for both the air- and water-quenched samples were derived from the classical parabolic equation<sup>46</sup>  $\Delta m^2 = k_p t + C$  (where  $\Delta m$  = specific mass gain,  $t$  = exposure time, and  $C$  is the intercept from the graph). The values were compared with those obtained from Pt-10Al-4Cr and Pt-10Al-4Ru alloys<sup>43</sup> in Table I.

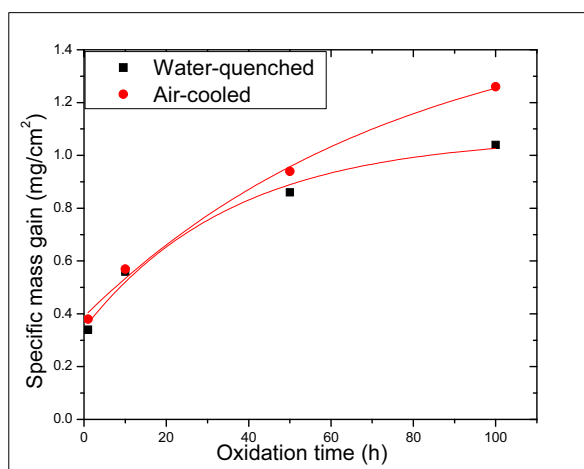


Figure 2—Specific mass gain for water-quenched and air-cooled Pt-11Al-3Cr-2Ru (at.%) specimens after isothermal oxidation in air at 1350°C [45]

**Table I-Properties of the different alloys (w = water quenched; a = air quenched; \* after 1000 h)-<sup>45</sup>**

Composition (at.%)	Exposure range (h)	$k_p$ ( $\text{mg}^2 \cdot \text{cm}^{-4} \cdot \text{h}$ )	Behaviour	$k_{ps}$ ( $\mu\text{m}^2 \cdot \text{h}$ )	Behaviour
Pt-10Al-4Cr <sup>43</sup>	1-100	0.005	Parabolic	1.3467	Parabolic
Pt-10Al-4Ru <sup>43</sup>	1-100	0.006	Linear	0.7159 *	Parabolic
Pt-11Al-3Cr-2Ru (w)	1-100	0.006 ± 0.0004	Parabolic	1.55 ± 0.01	Parabolic
Pt-11Al-3Cr-2Ru (a)	1-100	0.1 ± 0.0014	Parabolic	2.10 ± 0.007	Parabolic

The surface oxide grain size increased with oxidation time (Figure 3), with the pores becoming less discernable, as more and larger flakes formed<sup>45</sup>. The pores were deduced to arise from the way the oxide grains grew together unevenly. Oxide grains of approximately  $1.63 \pm 0.6 \mu\text{m}$  had grown after 100 hours. The oxide grains in the air-cooled samples were more rounded and joined (Figure 4).



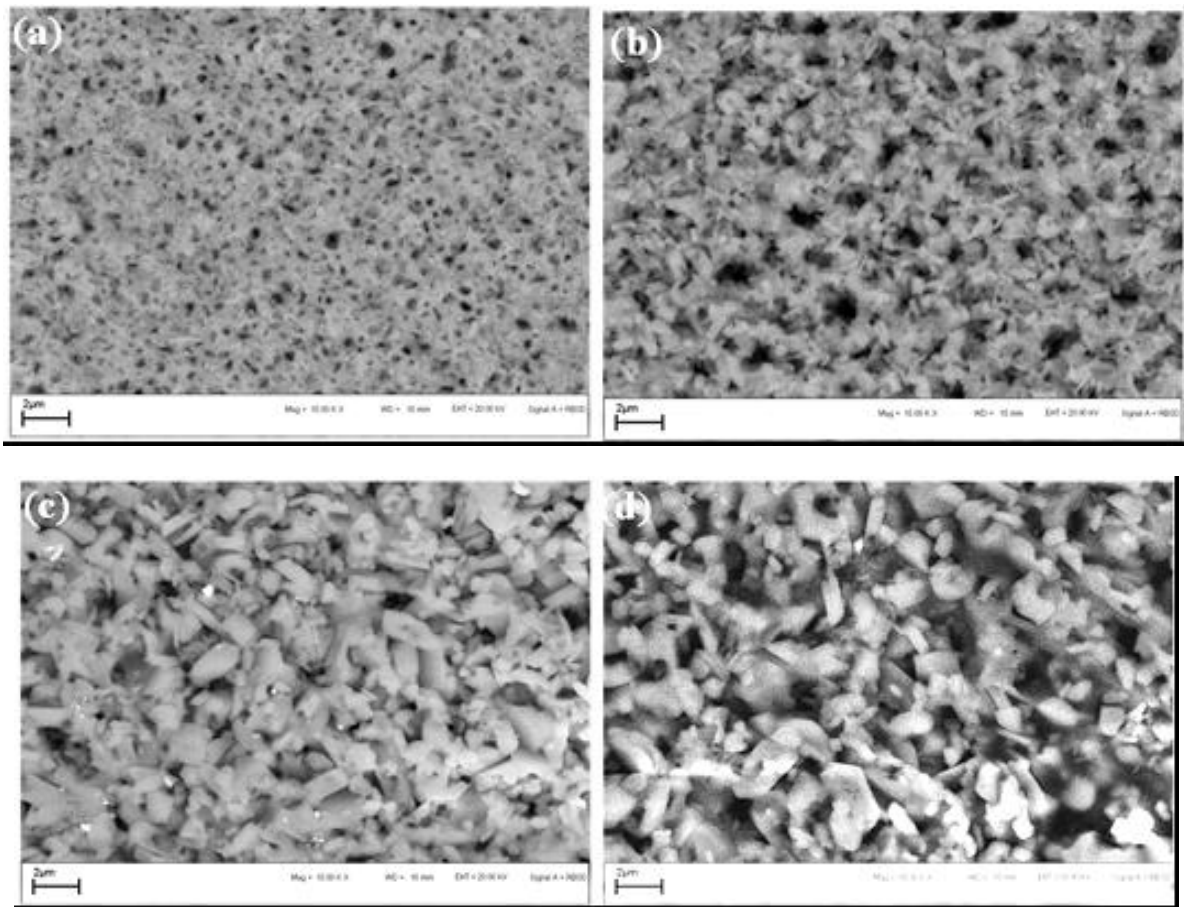


Figure 3—SEM-BSE images of the surface of water-quenched Pt-11Al-3Cr-2Ru (at.%) specimens after isothermal oxidation in air at 1350°C for: (a) 1 h, (b) 10 h, (c) 50 h and (d) 100 h<sup>45</sup>

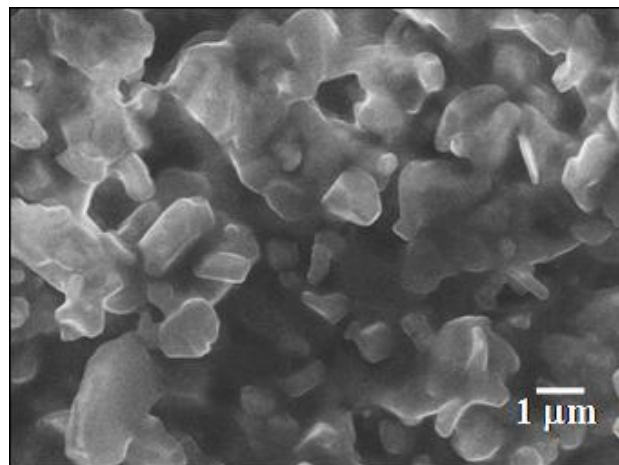
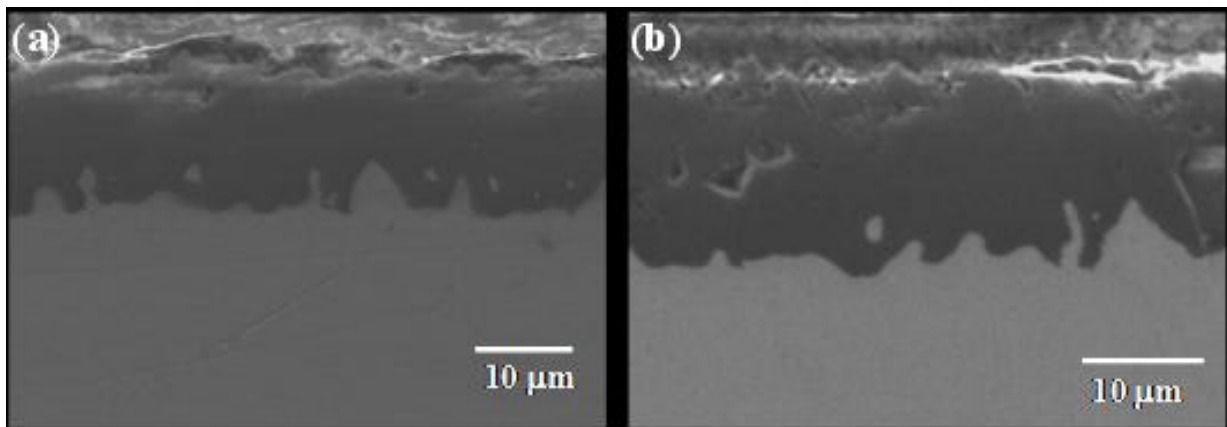


Figure 4—SEM-SE image of the surface of air-cooled Pt-11Al-3Cr-2Ru (at.%) specimen after 100 h oxidation in air at 1350°C<sup>45</sup>

The SEM-SE cross-sections (Figure 5) showed that the scales after oxidation at 1350°C were continuous with limited porosity<sup>45</sup>. X-ray elemental mapping of the scale after 100 hours' oxidation showed that the scale comprised mainly Al and O, which was confirmed by XRD. Scale thickness increased with oxidation time for both quenching media. Air-cooled specimens formed thicker scales than the water-quenched specimens, although high errors showed the differences were minor. The scales were also non-uniform in thickness, with irregular scale-substrate and scale-gas interfaces, which had no apparent relationship to each other (Figure 5). No zones of discontinuous oxides or any internal oxidation were observed, unlike similar alloys<sup>17</sup>. Beneficially, there was no void formation at the scale-alloy substrate interface, indicating that the scales were potentially protective.

The ridges or intrusions of oxide scale increased with exposure time. The oxide scales were also observed to protrude outwards at the scale-gas interface. The presence of substrate in the scale was deduced to be due to continuous lateral growth of the oxide after protrusion.



**Figure 5—SEM-BSE images of cross sections of Pt-11Al-3Cr-2Ru (at.%) specimens after 100 h oxidation in air at 1350°C (a) water-quenched (b) air-cooled<sup>45</sup>**

The irregular oxide-alloy interfaces improved the adhesion of the scale, due partially to mechanical keying<sup>47</sup>, although deleterious cavity formation at ridges associated with Pt-Al grain boundaries has been reported<sup>48-49</sup>. The high Pt content of the quaternary alloy may have improved the scale adherence, due to various mechanisms discussed by Reed *et al.*<sup>50</sup>.

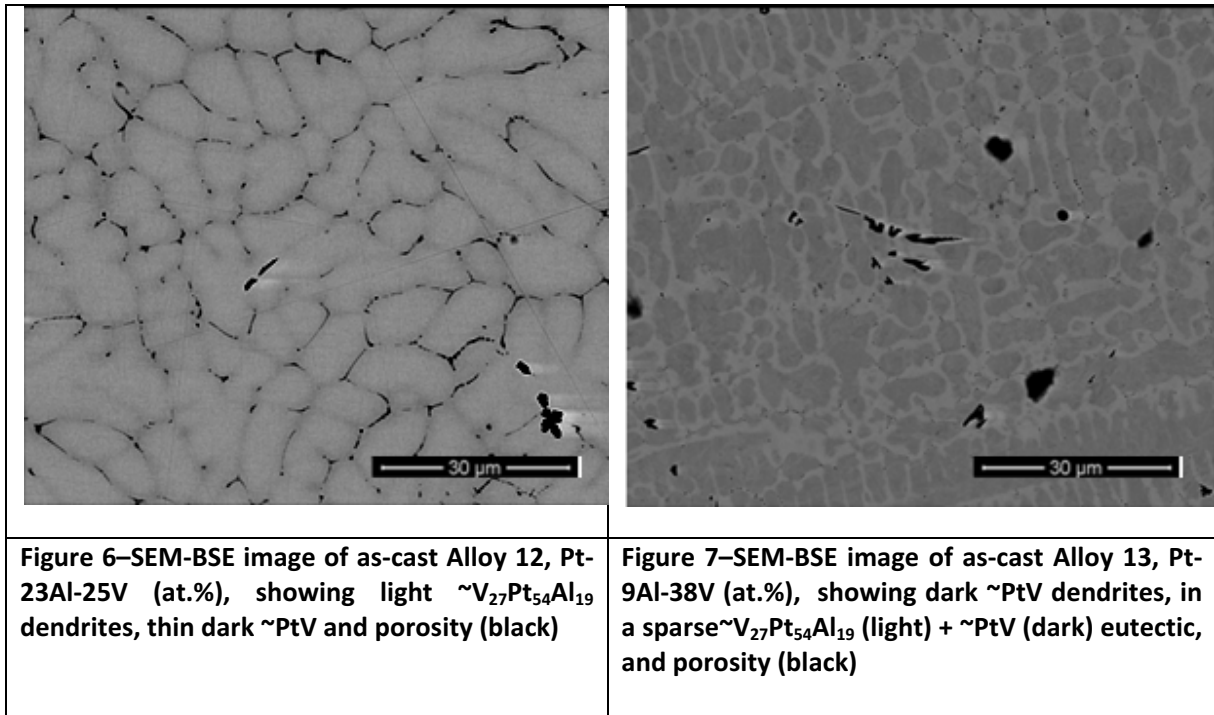
Future work to be reported will include the measurement of stress in the scales, using Raman spectroscopy. The stress is important because it is one of the determining factors for the durability of the scales.

## Alloying with vanadium

Although platinum has many beneficial properties, its high price and density are disadvantageous, and if the same structure and reasonable chemical properties could be retained, alloying could reduce the Pt content and hence the cost and density. A beneficial addition is vanadium which has a solubility in (Pt) of up to approximately 20.5 at.% V at 700°C which increases with increasing temperature, reaching approximately 7 at.% V at 1720°C<sup>51</sup>. Thus, as well as decreasing cost and density, V has potential both as a solid-solution strengthener and to increase the melting temperature<sup>19</sup>. Except for this ongoing study<sup>52-54</sup>, there is no reported data for Pt-Al-V, and phase diagram work on the system was necessary to check the extents of the phases and existence of any ternary phases that might be detrimental. Knowledge of the phases will help in defining the compositions of developmental alloys in the Pt-Al-Cr-Ru-V system.

Nine different Pt-Al-V composition alloys were manufactured by arc-melting under argon, with a titanium oxygen-getter, and sectioned. One half was prepared metallographically, then characterized using SEM with EDX, with XRD used for phase confirmation. The second half was annealed and will be reported in a later paper.

As expected, the alloys had very different microstructures, even from those reported earlier<sup>54</sup>. For example, Alloy 1<sup>54</sup>, average overall composition Pt-27Al-9V (at.%), had  $\sim$ Pt<sub>3</sub>Al dendrites,  $\sim$ Pt<sub>5</sub>Al<sub>3</sub> needles, a thin  $\sim$ Pt<sub>3</sub>V layer on the dendrites, and a complex eutectic-like microstructure. This consisted of  $\sim$ PtAl + Pt<sub>5</sub>Al<sub>3</sub> +  $\sim$ Pt<sub>5</sub>Al<sub>3</sub>, and resulted from the eutectic reaction  $L \rightarrow \beta + \sim$ Pt<sub>5</sub>Al<sub>3</sub> followed by the eutectoid decomposition  $\beta \rightarrow \sim$ PtAl +  $\sim$ Pt<sub>5</sub>Al<sub>3</sub>. Some of the later alloys had a ternary phase (Figure 6). An interesting example was Alloy 13, average overall composition Pt-9Al-38V (at.%), which had  $\sim$ PtV dendrites in a sparse eutectic comprising  $\sim$ V<sub>30</sub>Pt<sub>56</sub>Al<sub>14</sub> (a ternary phase) +  $\sim$ PtV (Figure 7).



A solidification projection of all the samples to date was plotted (Figure 7), and the liquidus surface<sup>54</sup> was extended to show the liquidus surface for the ternary phase. These figures are very important because they identified the likely limit of the addition of V at which the (Pt)/ $\sim Pt_3Al$  microstructure will be retained. Thus, Figure 8 shows that the maximum V addition is probably around 15 at.%, otherwise the  $\sim Pt_3V$  phase will be obtained, and the liquidus<sup>54</sup> shows a slightly lower value. A series of quinary alloys based on Pt-12Al-Cr4-Ru2 (at.%) have been manufactured, and the as-cast alloys show mainly dendrites with little or no eutectic, which agrees with the liquidus surface<sup>54</sup>. Additionally, the ternary phase needs to be avoided, but this phase only appears at V contents higher than 17 at.%.

Although the structure has yet to be determined, it is likely to be brittle. The next stage is to conduct hardness tests on the remaining alloys, and also to heat treat and characterize all the Pt-Al-Cr-Ru-V alloys to ascertain the effect of different amounts of vanadium.

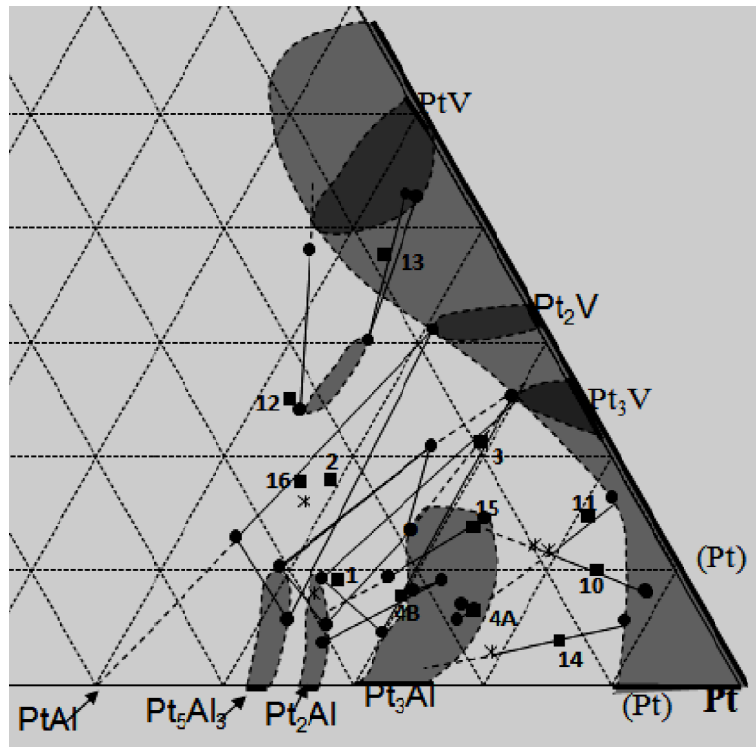


Figure 8—Solidification projection of the Pt-Al-V system above 50 at.% Pt

## Conclusions

Ongoing work on the Pt-based alloys has shown that microstructures much more like those of the NBSAs can be obtained with comparably high proportions of the strengthening  $\sim\text{Pt}_3\text{Al}$  precipitates, and the majority were the preferred cubic allotrope. Nano-indentation studies confirmed the higher hardness and Young's modulus of the  $\sim\text{Pt}_3\text{Al}$  compared to the (Pt) matrix. Recent work has shown that the oxide scale of Pt-11Al-3Cr-2Ru (at.%) up to 100 hours' exposure has potential for protection, and did not spall. There was no discernable Al depletion zone in the substrate, probably because it was greater than the depths of samples studied. The scales were at least as good as those of the ternary alloys.

Phase diagram work on the Pt-Al-V system has shown that there is a ternary phase of  $\sim\text{V}_{27}\text{Pt}_{54}\text{Al}_{19}$  (at.%) composition which has a eutectic reaction with (Pt). The maximum useful V addition is likely to be around 15 at.%, otherwise  $\sim\text{Pt}_3\text{V}$  or the ternary phase will form, and not the required (Pt)/ $\sim\text{Pt}_3\text{Al}$  phases.

### Acknowledgements

The Department of Science and Technology and the National Research Foundation are thanked for their support.

### References

1. Hill, P.J., Fairbank, G.B., and Cornish, L.A. New developments in high-temperature platinum alloys. *Journal of Metals*, vol. 53, no. 10, Oct. 2001. pp. 19-20.
2. Cornish, L.A., Hohls, J., Hill, P.J., Prins, S., Süß, R., and Compton, D.N. The development of platinum-based alloys and their thermodynamic database. *Journal of Mining and Metallurgy*, vol. 38, no. 3-4 B, 2002. pp. 197-204.
3. Cornish, L.A., Fischer, B., and Voelkl, R. Development of platinum group metal based superalloys for high temperature use. *Materials Research Society Bulletin*, vol. 28, no. 9, 2003. pp. 632-638.
4. Cornish, L.A., Süß, R., Völkl, R., Wenderoth, M., Vorberg, S., Fischer, B., Glatzel, U., Douglas, A., Chown, L.H., Murakumo, T., Preussner, J., Lupton, D., Glaner, L., Maledi, N.B., Potgieter, J.H., Sephton M., and Williams, G. Overview of the development of new Pt-based alloys for high temperature application in aggressive environments. *Journal of the Southern African Institute of Mining and Metallurgy*, vol. 107, no. 11, 2007. pp. 697-712.
5. Cornish, L.A., Süß, R., Douglas, A., Chown, L.H., and Glaner, L. The Platinum Development Initiative: Platinum-based alloys for high temperature and special applications: Part I. *Platinum Metals Review*, vol. 53, no. 1, 2009. pp. 2-10.
6. Douglas, A., Hill, P.J., Cornish, L.A., and Süß, R. The Platinum Development Initiative: Platinum-based alloys for high temperature and special applications: Part II. *Platinum Metals Review*, vol. 53, no. 2, 2009. pp. 69-77.
7. Cornish, L.A., Süß, R., Chown, L.H., and Glaner, L. The Platinum Development Initiative: Platinum-based alloys for high temperature and special applications: Part III. *Platinum Metals Review*, vol. 53, no. 3, 2009. pp. 155-163.
8. Hüller, M., Wenderoth, M., Vorberg, S., Fischer, B., Glatzel, U., and Völkl, R. Optimization of composition and heat treatment of age-hardened Pt-Al-Cr-Ni alloys. *Metallurgical and Materials Transactions A*, vol. 36A, no. 3A, 2005. pp. 681-689.
9. Vorberg, S., Wenderoth, M., Glatzel, U., Fischer, B., and Völkl, R. Pt-Al-Cr-Ni superalloys: heat treatment and microstructure. *JOM*, vol. 56, no. 9, 2004. pp. 40-43.

10. Vorberg, S., Wenderoth, M., Glatzel, U., Fischer, B., and Völkl R. A TEM investigation of the  $\gamma/\gamma'$  phase boundary in Pt-based superalloys. *JOM*, vol. 57, no. 3, Mar. 2005. pp. 49–51.
11. Völkl, R., Wenderoth, M., Preussner, J., Vorberg, S., Fischer, B., and Glatzel, U., A review on the progress towards Pt-base superalloys for ultra high temperature applications. *Platinum Surges Ahead*, Sun City, South Africa, 8 – 12 Oct. 2006. Symposium series S45. Southern African Institute of Mining and Metallurgy, Johannesburg. pp. 67-71,.
12. Wenderoth, M., Völkl, R., Vorberg, S., Fisher, B., and Glatzel, U. [Isothermal oxidation behavior of a precipitation-hardened Pt-base alloy with additions of Al, Cr and Ni](#), *International Journal of Materials Resources*, vol. 98, 2007. pp. 463-467.
13. Wenderoth, M., Cornish, L.A., Süß, R., Vorberg, S., Fischer, B., and Glatzel, U. On the development and investigation of quaternary Pt-based superalloys with Ni additions. *Metallurgical And Materials Transactions A*, vol.36 A, 2005. pp. 567-575.
14. Cornish, L.A., Süß, R., Watson, A., Preussner, J., Prins, S.N., Wenderoth, M., Völkl, R., and Glatzel, U. Building a database for the prediction of phases in Pt-based superalloys. *Journal of the Southern African Institute of Mining and Metallurgy*, vol. 107, no. 11, 2007. pp. 713-724.
15. Süß, R., Freund, D., Völkl, R., Fischer, B., Hill, P.J., Ellis, P., and Wolff, I.M. The creep behaviour of platinum-based  $\gamma/\gamma'$  analogues of nickel-based superalloys at 1300°C. *Materials Science and Engineering A*, vol. 338, no. 1-2, 2002. pp. 133.
16. Völkl, R., Yamabe-Mitarai, Y., Huang, C., and Harada, H. Stabilizing the L1<sub>2</sub> structure of Pt<sub>3</sub>Al(r) in the Pt Al-Sc system. *Metallurgical and Materials Transactions A*, vol. 36, 2005. pp. 2881–2892.
17. Wenderoth, M., Völkl, R., Yokokawa, T., Yamabe-Mitarai, Y, and Harada, H. High temperature strength of Pt-base superalloys with different  $\gamma'$  volume fractions. *Scripta Materialia*, vol. 54, 2006. pp. 275–279.
18. National Institute for Materials Science (NIMS). Research and development of superalloys for aeroengine applications. [http://sakimori.nims.go.jp/topics/hightemp\\_e.pdf](http://sakimori.nims.go.jp/topics/hightemp_e.pdf) [accessed 5 May 2010]
19. Massalski, T.B. Binary Phase Diagrams. ASM International, Ohio, USA, 1990.
20. Wolff, I.M. and Hill, P.J. Platinum metals-based intermetallics for high-temperature service. *Platinum Metals Review*, vol. 44, no. 4, 2000, pp. 158-166.

21. Potgieter, J.H., Maledi, N.B., Sephton, M. and Cornish, L.A. The Platinum Development Initiative: Platinum-based alloys for high temperature and special applications: Part IV, corrosion. *Platinum Metals Review*, vol. 54, no. 2, 2010. pp. 112-119.
22. Hill, P.J., Cornish, L.A., Ellis, P., and Witcomb, M.J. The effect of Ti and Cr additions on the phase equilibria and properties of (Pt)/Pt<sub>3</sub>Al alloys. *Journal of Alloys and Compounds*, vol. 322, 2001. pp. 166-175.
23. Mwamba, A. and Süß, Characteristics of platinum-base superalloy compacts produced via mechanical alloying. *Proceedings of the Microscopy Society of Southern Africa*, vol. 39, no. 57, 2009. p. 57.
24. C.T. Sims, C.T., Stoloff, N.S., and Hagel, W.C. *Superalloys II: High Temperature Materials for Aerospace and Industrial Power*. Wiley Inter-Science, New York, 1987.
25. McAlister, A.J. and Kahan, D. J The Al-Pt (aluminium-platinum) system. *Bulletin of Alloy Phase Diagrams*, vol. 7, 1986. pp. 45-51.
26. Oya, Y., Mishima, U., and Suzuki, T. Pt-Al and Pt-Ga phase diagram with emphasis on the polymorphism of Pt<sub>3</sub>Al and Pt<sub>3</sub>Ga. *Zeitschrift für Metallkunde*, vol. 78, no. 7, 1987. pp. 485-490.
27. Hill, P.J., YAMABE-MITARAI, Y., MURAKAMI, H., CORNISH, L.A., WITCOMB, M.J., WOLFF, I.M., and HARADA, H. The precipitate morphology and lattice mismatch of ternary (Pt)/Pt<sub>3</sub>Al alloys. *Structural Intermetallics 2001*. Hemker, K.J. (ed.). TMS, 2001. pp. 527-533.
28. Shongwe, M.B. Optimisation of compositions and heat treatments of Pt-based superalloys. M.Sc. Dissertation, University of the Witwatersrand, 2009.
29. Shongwe, M.B., Cornish, L.A., and Süß, R. Improvement of ~Pt<sub>3</sub>Al volume fraction and hardness in a Pt-Al-Ru-Cr Pt-based superalloy. *Advanced Metals Initiative Conference*, Gold Reef City, Johannesburg, 18 - 19 November 2008 [on CD].
30. Shongwe, M.B., Odera, B., Samal, S., Ukpong, A.M., Watson, A., Süß, R., Chown, L.H., Rading, G.O., and Cornish, L.A. Assessment of microstructures in the development of Pt-based superalloys. *Light Metals 2012*, Mist Hills Conference Centre, Cradle of Humankind, Gauteng, South Africa, 27-29 October 2010. Southern African Institute of Mining and Metallurgy, Johannesburg, 2010.



31. Shongwe, M.B., Cornish, L.A., and Süß, R. Improvement of  $\sim\text{Pt}_3\text{Al}$  volume fraction and hardness in a Pt-Al-Ru-Cr Pt-based superalloy. *Advanced Metals Initiative Conference*, Gold Reef City, Johannesburg, 18 - 19 November 2008 [on CD].
32. Shongwe, M.B., Odera, B., Samal, S., Ukpong, A.M., Watson, A., Süß, R., Chown, L.H., Rading, G.O., and Cornish, L.A. Assessment of microstructures in the development of Pt-based superalloys. *Light Metals Conference*, Muldersdrift, Johannesburg, 27-29 October 2010 [on CD].
33. Shongwe, M.B., Witcomb, M.J., Cornish, L.A., and Papo, M.J. TEM investigation of  $\sim\text{Pt}_3\text{Al}$  precipitate morphology and volume fraction of  $\text{Pt}_{82}:\text{Al}_{12}:\text{Ru}_2:\text{Cr}_4$ . *Proceedings of the Microscopy Society of Southern Africa Conference*, Pretoria, South Africa, 4-9 December 2011. Vol. 41, p. 81,
34. Shongwe, M.B., Cornish, L.A., and Süß, R. Effect of misfit on the microstructure of Pt based superalloys. *Proceedings of the Microscopy Society of Southern Africa Conference*, Durban, 8– 11 December 2009, vol. 39, p. 59.,
35. Shongwe, M.B., Cornish, L.A., Witcomb, M.J., and Papo, J.M. TEM studies of quaternary Pt-based superalloys, ZrTa. *2011 New Metals Development Network Conference*, 13-14 October 2011, Magaliesburg, South Africa. Abstracts, p. 56, [on CD].
36. Witcomb, M.J. Preparation of Pt and Pt-C foils for conventional and atomic resolution TEM. *Proceedings of the Electron Microscopy Society of Southern Africa* vol. 22, 1992. pp. 39-40.
37. Murr, L.E. *Electron Optical Applications in Materials Science*. McGraw-Hill, New York, 1970.
38. Loretto, M.H. and Smallman, R.E. *Defect Analysis in Electron Microscopy*, T. & A. Constable, Edinburgh, 1975.
39. Huch, R. and Klemm, W. The platinum-aluminium system. *Zeitschrift für Anorganische und Allgemeine Chemie*, vol. 329, 1964. pp. 123-135.
40. Durst, K. and Göken, M. Micromechanical characterisation of the influence of rhenium on the mechanical properties in nickel base superalloys. *Materials Science and Engineering A*, vol. 387–389, 2004. pp. 312–316.

41. Nikulina, E., Durst, K., Göken, M., Völkl, R., and Glatzel, U. Microstructural and micromechanical characterisation of a Pt-Al-Cr-Ni-Re alloy. *International Journal of Materials Research*, vol. 101, no. 5, 2010. pp. 585-588.
42. Hill, P.J., Cornish, L.A., Witcomb, M.J., and Wolff, I.M. The oxidation behaviour of Pt-Al alloys at temperatures between 1473 and 1623 K. *Proceedings of the International Symposium on High Temperature Corrosion and Protection*, Hokkaido, Japan. *Science Reviews*, vol. 185, 2000.
43. Süß, R., Hill, P.J., Ellis, P., and Wolff, I.M. The oxidation resistance of Pt-based  $\gamma/\gamma'$  analogues to Ni-based superalloys. *Proceedings of the 7th European Conference on Advanced Materials and Processes*, Rimini, Italy, 10-14 June, 2001. Paper no. 287 [on CD-ROM, ISBN 8885298397].
44. Süß, R., Hill, P.J., Ellis, P., and Cornish, L.A. The oxidation resistance of Pt-base superalloy Pt<sub>80</sub>:Al<sub>14</sub>:Cr<sub>3</sub>:Ru<sub>3</sub> compared to that of Pt<sub>86</sub>:Al<sub>10</sub>:Cr<sub>4</sub>. *Proceedings of the Microscopy Society of Southern Africa*, vol. 31, no. 21, 2001. p. 31.
45. Odusote, J.K., Cornish, L.A., Chown, L.H., and Erasmus, R.M. Isothermal oxidation behaviour of a two-phase  $\gamma/\gamma'$  precipitation-hardened quaternary Pt-based alloy in air at 1350°C. *Oxidation of Metals*, in press.
46. Kubaschewski O. and Hopkins, B.E. *Oxidation of Metals and Alloys*, 2nd edn. Butterworths, London, 1962.
47. Felten E.J. and Pettit, F.S. Development, growth and adhesion of Al<sub>2</sub>O<sub>3</sub> on platinum-aluminium alloys. *Oxidation of Metals*, vol. 10, no. 3, 1976. pp. 189-223.
48. Gell, M., Jordan, E., Vaidyanathan, K., McCarron, K., Barber, B., Sohn Y.-H., and Tolpygo, V.K. Bond strength, bond stress and spallation mechanisms of thermal barrier coatings. *Surface Coatings Technology*, vol. 120-121, 1999. pp. 53-60
49. Gell, M., Vaidyanathan, K., Barber, B., Cheng, J., and Jordan, E. Mechanism of spallation in platinum aluminide/electron beam physical vapour deposited thermal barrier coatings. *Metallurgical Transactions A*, vol. 30, 1999. pp. 427-435.
50. Reed, R.C., Wu, R.T., Hook, M.S., Rae, C.M.F., and Wing, R.G. On oxidation behaviour of platinum aluminide coated nickel based superalloy CMSX-4, *Materials Science and Technology*, vol. 25, 2009. pp. 277-286.
51. Waterstrat, R.M. The vanadium-platinum constitution diagram. *Metallurgical Transactions*, vol. 4, 1973. pp. 455.

52. Odera, B.O., Cornish, L.A., Suss, R., and Rading, G.O. A study of phases in as-cast alloys from the Pt-Al-V system at the Pt-rich corner. *Proceedings of the Microscopy Society Of Southern Africa.*, Durban, South Africa, vol. 39, 2009. pp. 61.
53. Odera, B.O., Cornish, L.A., Rading, G.O., and Papo M.J. Solidification projection of the Pt-Al-V system at the Pt-rich corner. *Proceedings of the Microscopy Society Of Southern Africa*, vol. 41, 2011 pp. 72.
54. Odera, B.O., Cornish, L.A., Shongwe, M.B., Rading, G.O., and Papo, J.M. As-cast and heat treated alloys of the Pt-Al-V system at the Pt-rich corner. *Journal of the Southern African Institute of Mining and Metallurgy*, in press.

### The Author



**Bernard Odera**, *Student*, University of the Witwatersrand

PhD Student, School of Chemical and Metallurgical Engineering, University of the Witwatersrand, 2009 to Present

Lecturer, University of Nairobi, 1987 to Present

